

ADVANCED ELECTRONIC MATERIALS

Supporting Information

for *Adv. Electron. Mater.*, DOI: 10.1002/aelm.202001114

Green fabrication of (6,5)CNT/protein transistor endowed
with specific recognition

*Marcello Berto, Matteo Di Giosia, Martina Giordani, Matteo Sensi,
Francesco Valle, Andrea Alessandrini, Claudia Menozzi, Andrea
Cantelli, G. Carlo Gazzadi, Francesco Zerbetto, Matteo Calvaresi*,
Fabio Biscarini and Carlo A. Bortolotti**

SUPPORTING INFORMATION

Green fabrication of (6,5)CNT/protein transistor endowed with specific recognition

Marcello Berto, Matteo Di Giosia, Martina Giordani, Matteo Sensi, Francesco Valle, Andrea Alessandrini, Claudia Menozzi, Andrea Cantelli, G. Carlo Gazzadi, Francesco Zerbetto, Matteo Calvaresi, Fabio Biscarini and Carlo A. Bortolotti**

Dr. M. Berto, Dr. M. Giordani, Dr. M. Sensi, Prof. F. Biscarini, Dr. C.A. Bortolotti
Dipartimento di Scienze della Vita - Università di Modena e Reggio Emilia, Via Campi 103, Modena 41125, Italy
Email: carloaugusto.bortolotti@unimore.it

Dr. Matteo Di Giosia, Dr. A. Cantelli, Prof. Francesco Zerbetto, Prof. Matteo Calvaresi
Dipartimento di Chimica “Giacomo Ciamician”, Alma Mater Studiorum - Università di Bologna, Via Francesco Selmi 2, 40126 Bologna, Italy
Email: matteo.calvaresi3@unibo.it

Dr. F. Valle
CNR - Istituto per lo Studio di Materiali Nanostrutturati, Via P. Gobetti, 101, 40129, Bologna, Italy

Dr. F. Valle
Consorzio Interuniversitario per lo Sviluppo dei Sistemi a Grande Interfase (CSGI), via della Lastruccia 3, 50019 Firenze, Italy

Prof. A. Alessandrini, Dr. C. Menozzi, Dr. G.C. Gazzadi
CNR - Istituto Nanoscienze, S3, Via Campi 213/A, 41125, Modena, Italy

Prof. A. Alessandrini, Dr. C. Menozzi
Dipartimento di Scienze Fisiche, Informatiche e Matematiche, Università di Modena e Reggio Emilia, Via Campi 213/A, 41125, Modena, Italy

Prof. F. Biscarini
Center for Translational Neurophysiology - Istituto Italiano di Tecnologia
Via Fossato di Mortara 17-19, Ferrara 44100, Italy

Contents:

- 1. Experimental Section**
- 2. Computational Details**
- 3. Figures and table**
- 4. References**

Experimental Section

Materials

Single-walled semiconducting carbon nanotube (95%), enriched in (6,5) chirality, produced using CHASM's patented CoMoCAT™ synthesis technology (code 773735), and lysozyme (from chicken egg white, code L6876) were obtained from Sigma-Aldrich.

LZ/(6,5)CNT synthesis and characterization

Proteins-CNT hybrids were prepared by addition of 1.5 mg of CNT powder, used as commercially available, without any additional purification, in a 3 mg/ml solution (1 ml) of protein in Milli-Q water. After sonication for 60 min using a probe tip sonicator (Hielscher Ultrasonic Processor UP200St, equipped with a sonotrode S26d7, used at 40% of the maximum amplitude) in an ice bath, CNTs were dispersed in the protein solution forming a black mixture. A black solution was obtained after centrifugation at 10000g for 10 min and collection of the supernatant.^[1]

UV-vis absorption spectra were recorded at 25 °C by means of Agilent Cary 60 UV-Vis Spectrophotometer.

Atomic Force Microscopy

(6,5)CNT both conjugated with lysozyme and with SDS were imaged in air by a Bioscope I AFM (Bruker) equipped with a Nanoscope IIIa controller and operated in Tapping mode. The samples were

diluted in milliQ water to a concentration suitable for imaging. LZ/(6,5)CNT and SDS/(6,5)CNT were, as much as possible isolated, then 5 μ l were spotted onto freshly cleaved mica and dried with a stream of N₂.

Images were collected at an average scan frequency of 1 line/s using NTMDT NSG10 tips with a nominal spring constant of 12 N/m.

LZ/(6,5)CNT EGT fabrication

The Silicon Test Patterns (TPs) (1 cm² as total area) were purchased from “Fondazione Bruno Kessler” (FBK, Trento, Italy). The silicon TPs feature four transistors: two of them have widths (W) and channel lengths (L) equal to 11.2 mm and 20 μ m, respectively; the remaining two maintain the same geometry (namely a W/L ratio of 560) with W = 22.4 mm and L = 40 μ m. The substrate is Silicon and the dielectric layer is a thermally grown 200 nm thick SiO_x layer. Source and Drain gold electrodes are patterned with interdigitated fingers of 150 nm thick by photolithography and lift-off. A thin adhesive layer of Cr (2 nm thick) is pre-patterned underneath the gold layer. The quartz ones were purchased from “MicroFabSolutions” (Trento, Italy); they feature four interdigitated electrodes with W/L ratio equal to 200 (two of them have channel length L = 15 μ m and channel width W = 3 mm, the other two have channel length L = 30 μ m and channel width W = 6 mm) patterned by photolithography and lift-off. The Source and Drain gold electrodes are 50 nm thick with few nm of chromium adhesive layer on quartz substrate (optical grade). The standard cleaning procedure is composed by: (i) rinsing with acetone (~10 ml) in order to remove the photoresist layer, (ii) drying with nitrogen flow, (iii) washing again in hot acetone for 15 min, and (iv) drying with nitrogen. A final rinse with water is done before the nanotube deposition. LZ/(6,5)CNT semiconductive layer has been deposited by drop casting 80 μ l of LZ/(6,5)CNT solution onto the cleaned test pattern. A rinse with water is done before the electrical characterization. Deposition of the semiconducting channel by spin coating or deposition of a drop of solution under application of a voltage difference were also attempted, but both methods yielded lower electrical performances.

Determination of the amount of lysozyme displayed on the (6,5)CNT semiconductive surface.

The quantification of lysozyme adsorbed on the (6,5)CNTs in the EGT device was carried out desorbing the proteins from the LZ/(6,5)CNT hybrids under denaturing conditions. 50 μl of the obtained LZ/(6,5)CNT solution was added to 950 μl of 10 M urea in a 2 ml Eppendorf tube. The mixture was heated at 97°C for 30 minutes under constant shaking at 700 rpm (Mixer HC – Starlab). During this step, due to protein unfolding and detachment from the CNT surface, the bare CNTs aggregate and coagulation phenomena occur. CNTs aggregates were separated from lysozyme solution by filtration with 0.2 μm syringe filter. The filtered solution was characterized by UV-Vis spectroscopy (Agilent Cary 60). Based on the extinction coefficient of lysozyme ($\epsilon^{280\text{nm}} = 38,940 \text{ M}^{-1}\text{cm}^{-1}$), the concentration of the protein adsorbed on the CNTs was determined to be 83 μM , corresponding to 40% of the initial amount of lysozyme used to disperse CNTs (3mg/ml; 208 μM). Considering the amount of solution used in the drop casting process, we can estimate that the number of proteins adsorbed on CNTs is $\sim 2.5 \cdot 10^{15}$ per device.

Electrical characterization

Electrical characterization was performed in phosphate buffer (PBS 50 mM, pH 7.4) with a Pt wire gate electrode. Source, drain, and gate electrodes were connected to an Agilent B2912A Source Meter Unit. All measurements were carried out at room temperature. The I–V transfer characteristics were performed by sweeping the gate-source voltage (V_{GS}) from 0.0 V to -0.5 V while leaving the drain-source voltage (V_{DS}) constant at -0.1 V (linear regime). The output characteristics were performed by sweeping V_{DS} from 0.0 V to -0.5 V and V_{GS} from 0 V to -0.5 V with steps of 0.1 V. Electrical measurements were acquired in buffered environment containing increasing NAG₃ concentration, ranging from 1 μM to 500 μM , under static conditions (i.e., not in a flow cell geometry). After each measurement in NAG₃ solutions, the device was thoroughly washed with buffer only. NAG₃ has been purchased from Megazyme (Ireland).

Scanning Electron Microscopy

Surface characterization has been performed with a Scanning Electron Microscope Zeiss Sigma equipped with a Schottky Field Emission Gun operating at 5 keV. Before to measure the LZ/(6,5)CNT layer thickness, to avoid deformation, the device has been immersed in liquid nitrogen (1 minute) and then cleaved.

Image analysis

Both AFM and SEM images were analyzed by Gwyddion where both standard operations such as flattening, zero setting or color scale and more advanced ones such as Power Spectrum Density Function (PSDF) calculation were performed.

One-dimensional PSD was used because of the isotropy of the features present in the SEM images of this work; PSD was obtained by transforming the image line by line along the fast scan direction and then averaging. The range of frequencies included in the analysis are between $k_{\min} = 1/L$ (L being the image size) and the Nyquist frequency $k_{\max} = N/(2L)$ (N being the number of pixels of the image).

Computational Details

Generation of the poses. Docking models were obtained using the PatchDock algorithm.^[2]

PatchDock takes as input two molecules and computes three-dimensional transformations of one of the molecules with respect to the other with the aim of maximizing surface shape complementarity, while minimizing the number of steric clashes. Given a protein and a molecule, PatchDock first divides their surfaces into patches according to the surface shape (concave, convex, or flat). Then, it applies the geometric hashing algorithm to match concave patches with convex patches and flat patches with flat patches and generates a set of candidate transformations. Each candidate transformation is further evaluated by a set of scoring functions that estimate both the shape complementarity and the atomic desolvation energy^[3] of the complex. These terms are the most

important in the case of binding of carbon nanotubes with proteins. Redundant solutions are discarded by use of rmsd (root-mean-square deviation) clustering. PatchDock is highly efficient, because it utilizes advanced data structures and spatial pattern detection techniques, which are based on matching of local patches. The local shape information is then extended and integrated to achieve global solutions. The algorithm implicitly addresses surface flexibility by allowing minor inter-penetrations of the molecules.

Scoring of the poses. Accurate rescoring of the complexes is then carried out using FireDock program.^[4] This method simultaneously targets the problem of flexibility and scoring of solutions produced by fast rigid-body docking algorithms. Possible readjustments of the protein structure in the presence of the solvent are accounted for. Redundant entries are present in the database for proteins known to be flexible, sidechain flexibility is modeled by rotamers and Monte Carlo minimization.^[5] Following the rearrangement of the side-chains, the relative position of the docking partners is refined by Monte Carlo minimization of the binding score function. Desolvation free energy in the binding process is taken into account by a solvation model using estimated effective atomic contact energies (ACE). All the candidates are ranked by a binding score.^[4] This score includes, in addition to atomic contact energy used to estimate the desolvation energies,^[3] van der Waals interactions, partial electrostatics, explicit hydrogen and disulfide bonds contribution. In addition, three additional components to the total binding score are added: $E_{\pi-\pi}$ for the calculation of the $\pi-\pi$ interactions, $E_{\text{cation}-\pi}$ for the calculation of the cation- π interactions and E_{aliph} for the calculation of hydrophobic interactions. These energetic components are crucial to describe:

- i) the interactions that occur between the aromatic residues Trp, Phe, Tyr, His, and the SWCNT wall surface
- ii) the interactions of the positive amines of Lys or Arg with the π -electron cloud of the SWCNTs (Phe, Tyr, Trp),
- iii) the hydrophobic interactions that involve aliphatic residues as Met, Leu, Ile, Pro, Val, Ala.

Figures and table

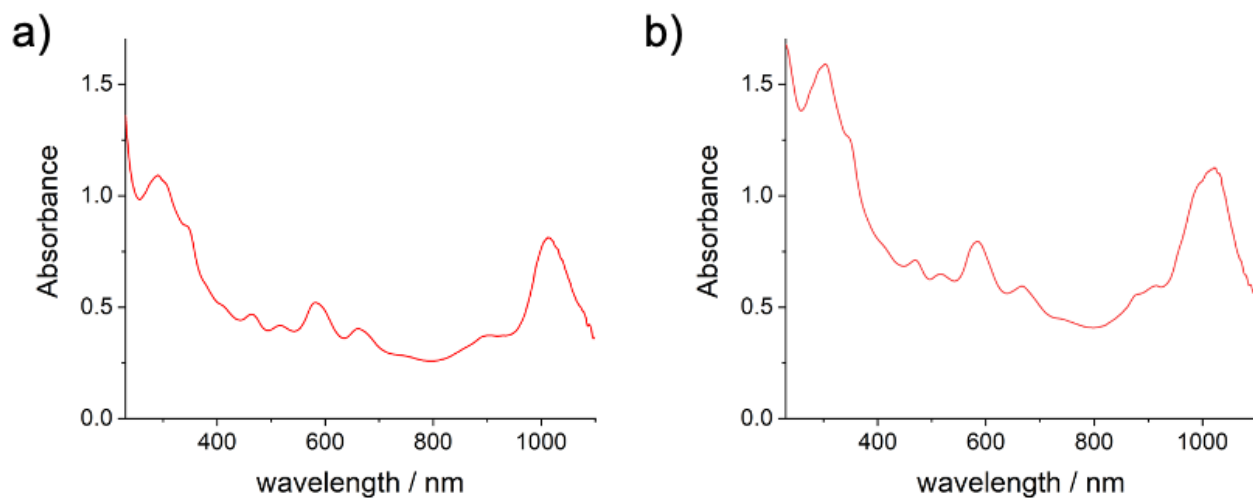


Figure S1. UV-vis-NIR absorption spectrum of dispersion of (6,5)CNT with (a) lysozyme and (b) SDS.

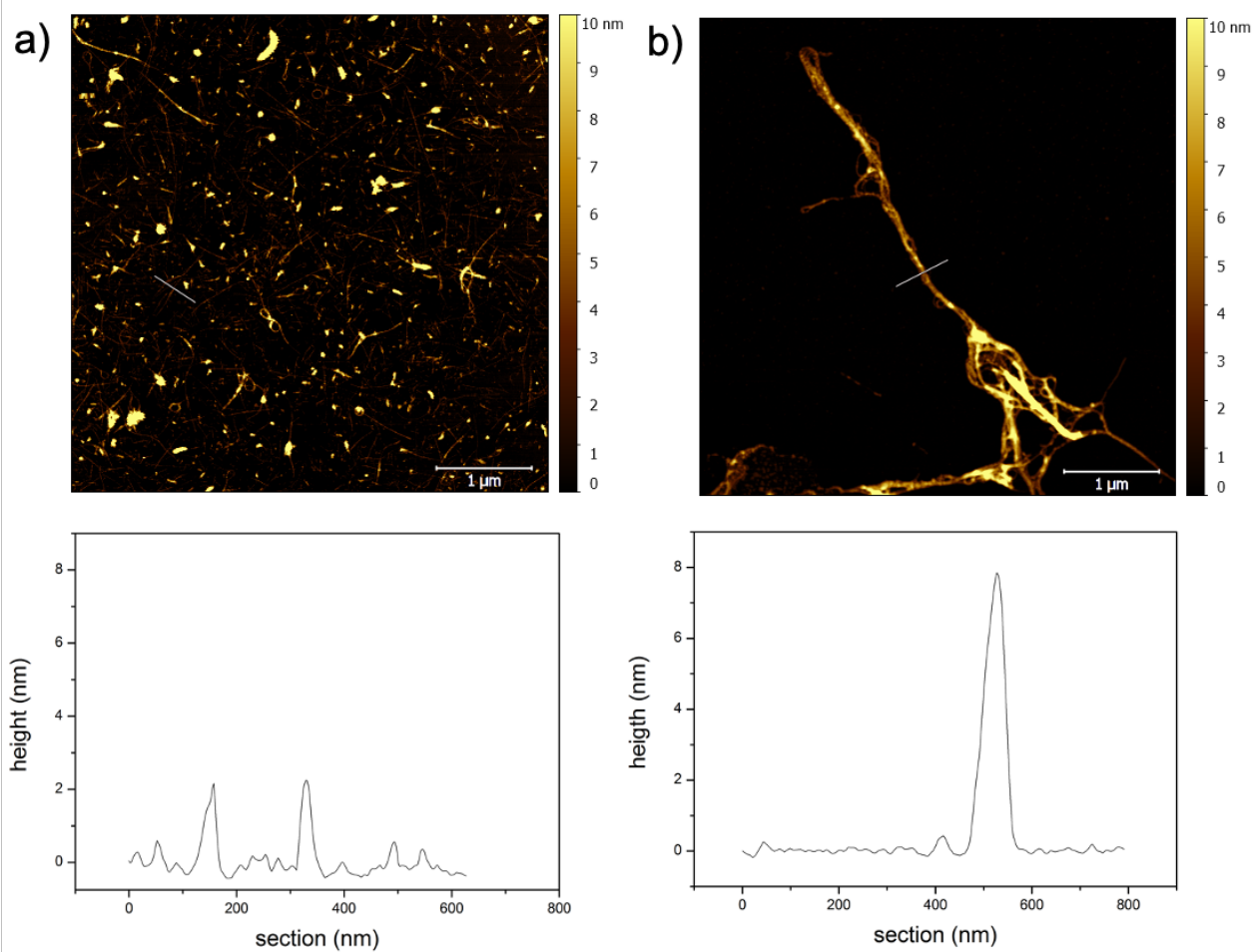


Figure S2. Top. AFM images of (a) LZ/(6,5)CNT and (b) SDS/(6,5)CNT dispersion. Bottom. Profile analysis: Left, profile of white line in Figure S2a; right, profile of white line in Figure S2b.

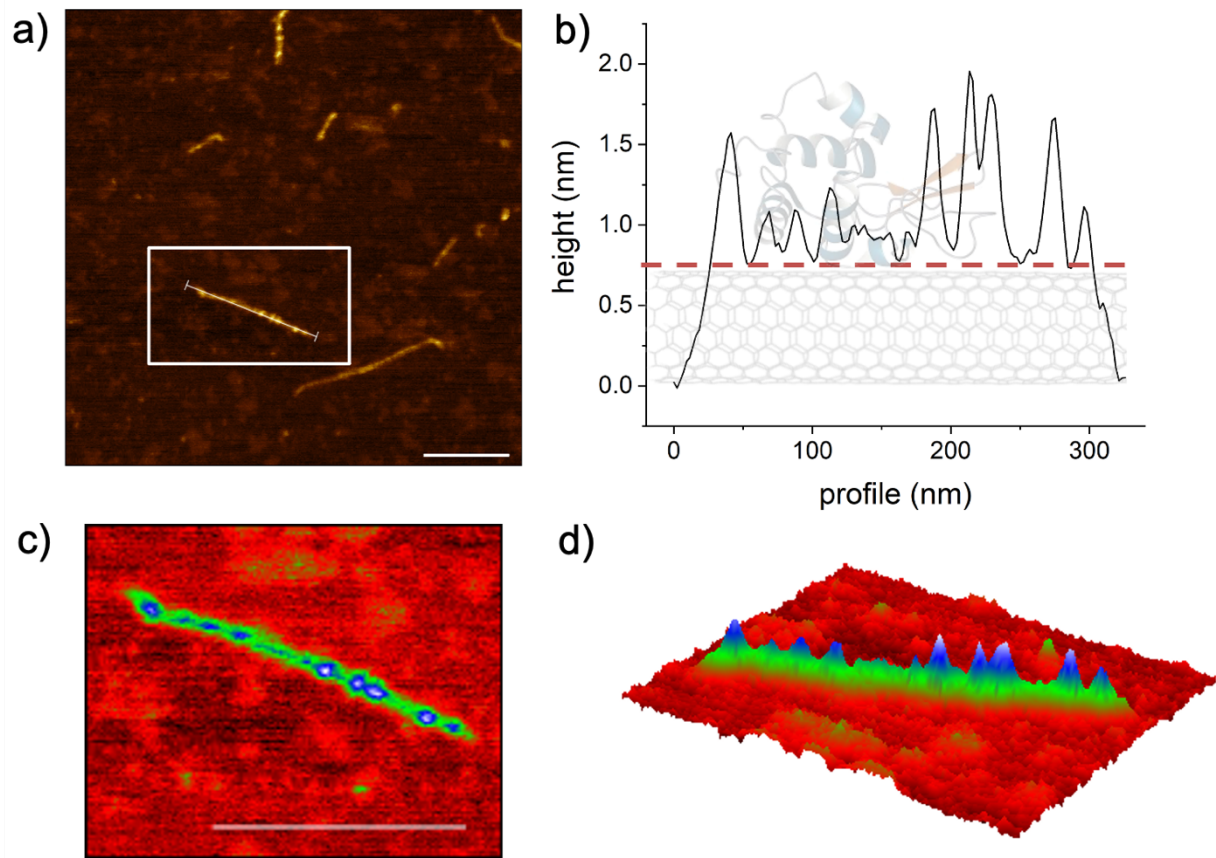


Figure S3. a) AFM images of LZ/(6,5)CNT. a) top view; b) profile analysis: profile indicated in Figure S3a (white line), c) magnification of the rectangular selection indicated in Figure S3a, top view d) 3D rendering of Figure S3c. Scale bars 200nm

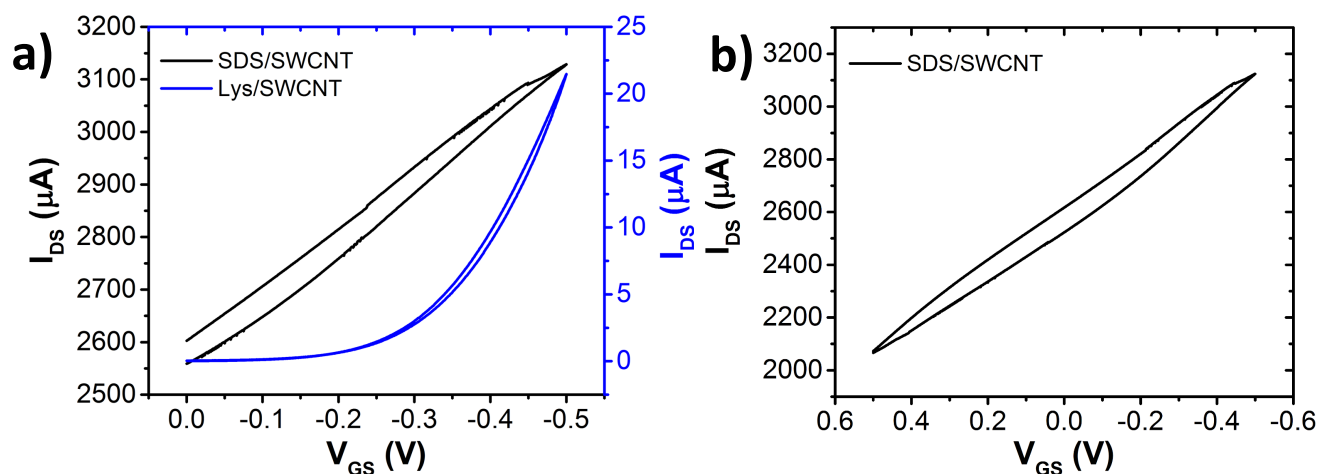


Figure S4. (a) Transfer characteristics of SDS/(6,5)CNT (black) and LZ/(6,5)CNT (blue) EGT on silicon ($V_{DS} = -0.1$ V, $V_{GS} = 0.0 \div -0.5$ V). (b) Ohmic electrical behavior of SDS/(6,5)CNT EGT moving from $V_{GS} = 0.5$ V to $V_{GS} = -0.5$ V.

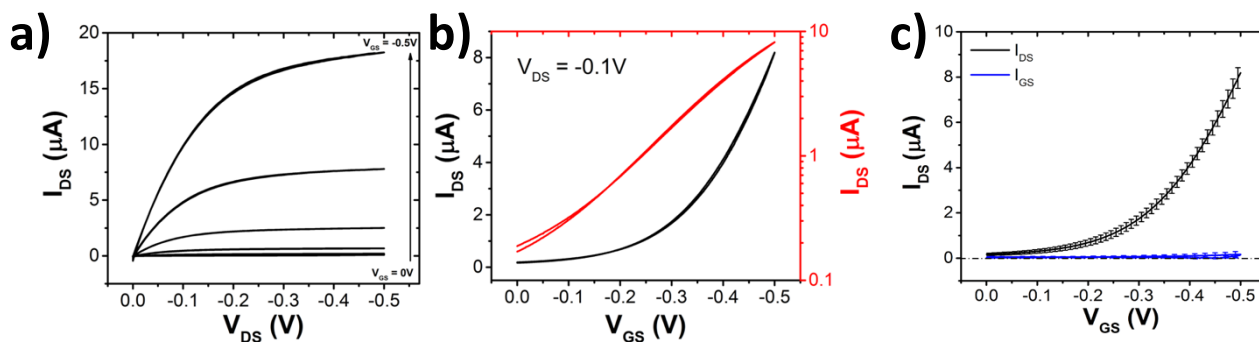


Figure S5. Electrical performance of LZ/(6,5)CNT EGT prepared from 1.50 $\mu\text{g}/\text{ml}$ solution: (a) output characteristics recorded for $I_{GS} = 0\text{V} \div -0.5\text{V}$; (b) lin-lin (black) and semilog (red) transfer characteristics; (c) average transfers characteristics recorded at $V_{DS} = -0.1$ V; in black the channel current I_{DS} , in blue the leakage current I_{GS} . Error bars correspond to the rms of the current averaged over ten devices.

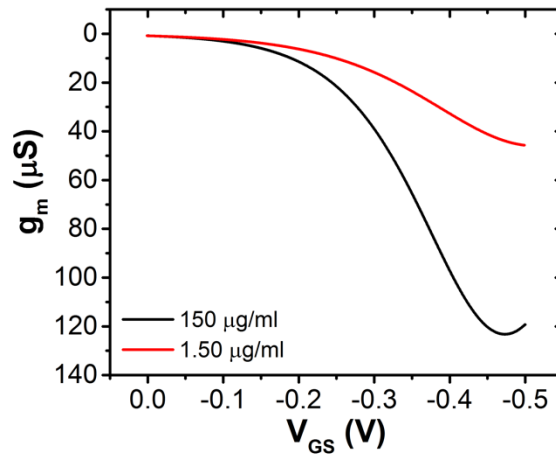


Figure S6. Transconductance g_m for LZ/(6,5)CNT EGT on silicon prepared from 1.50 $\mu\text{g/ml}$ solution (red curve) and 150 $\mu\text{g/ml}$ (black curve)

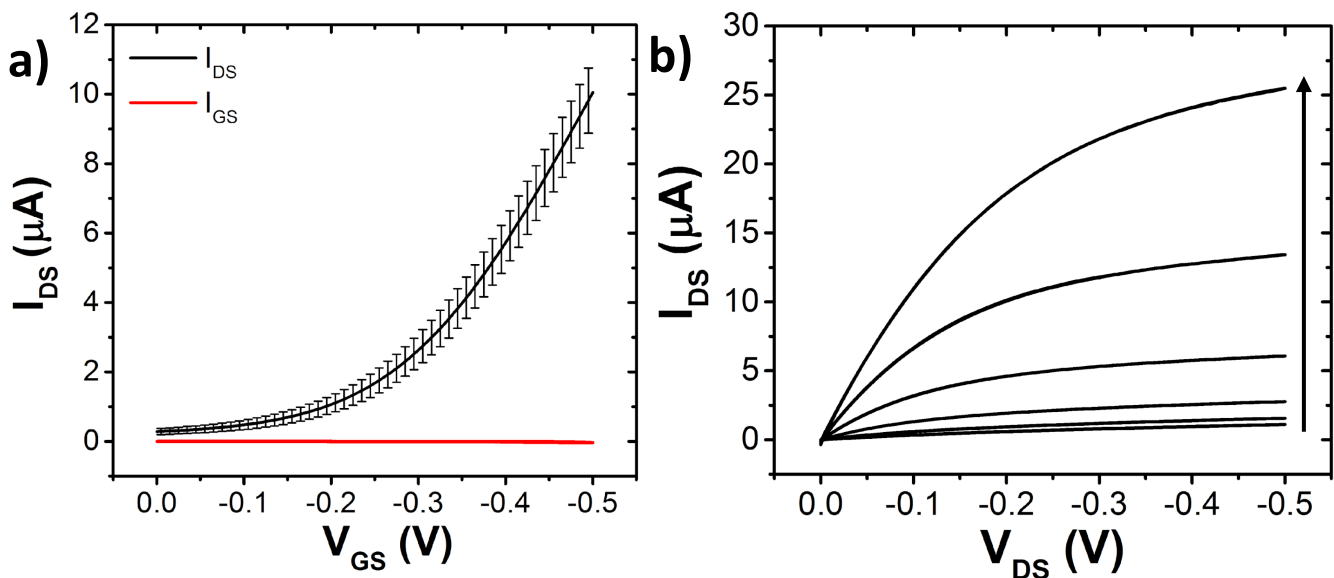


Figure S7. Electrical performances of LZ/(6,5)CNT EGT on quartz (prepared from 1.50 $\mu\text{g/ml}$ solution): (a) transfers characteristics recorded at $V_{DS} = -0.1\text{V}$ (linear regime); in black the channel current I_{DS} , in red the leakage current I_{GS} . Error bars correspond to the rms of the current averaged over fifteen devices; (b) output characteristics recorded for $V_{GS} = 0\text{V} \div -0.5\text{V}$.

Table S1. Average electrical parameters of LZ/(6,5)CNT EGTs*

Device	W/L	g_m (μS)	V_{th} (mV)	ON/OFF ratio
Silicon substrate (6,5)CNT 1.50 $\mu g/ml$	560	45 (± 2)	-317 (± 2)	80
Silicon substrate (6,5)CNT 150 $\mu g/ml$	560	137 (± 4)	-331 (± 10)	778
Quartz substrate (6,5)CNT 1.50 $\mu g/ml$	200	44 (± 2)	-275 (± 7)	40

* the associated errors are standard deviation of 10, 8, and 15 devices for data in rows a, b and c

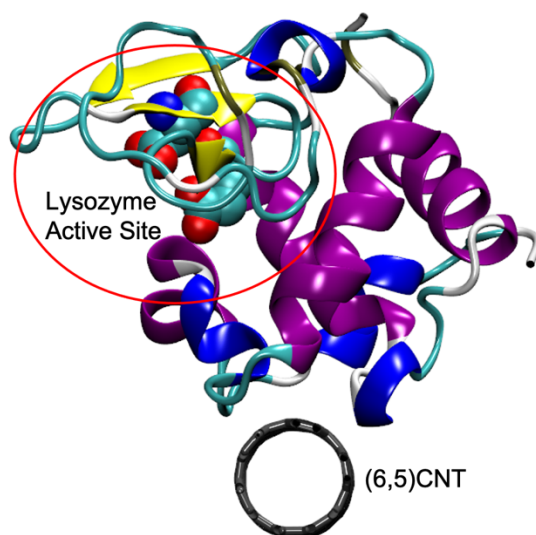


Figure S8. Interaction between (6,5)CNT and lysozyme. In van der Waals representation are the catalytic residues of the proteins (Asp52 and Glu35).

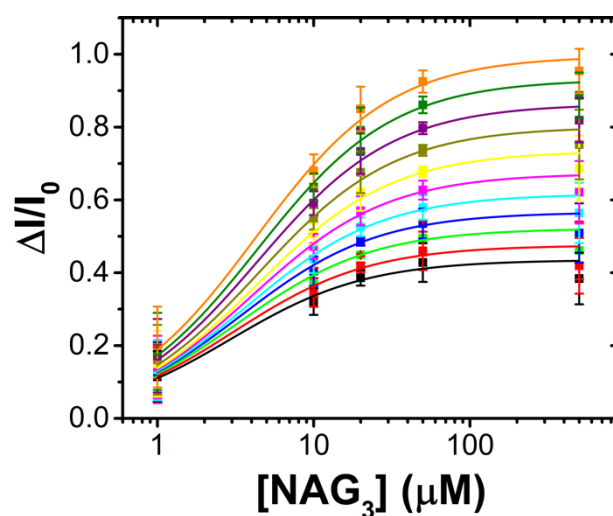


Figure S9. (a) Dose curves acquired at increasing gate voltages from $V_{GS} = -0.3$ V (top curve, orange) to $V_{GS} = -0.5$ V (bottom curve, black); each curve corresponds to a -20 mV variation. Error bars correspond to the signal averaged over five devices. The data are fitted with the Langmuir equation (equation 1 in the main text).

Table S2. K_d for the lysozyme/NAG₃ complex extracted at different V_{GS} (data from Figure S6).

K_d (μM)	V_{GS}
4.8 ± 0.3	-0.3 V
3.7 ± 0.6	-0.4 V
3.1 ± 0.8	-0.5 V

Table S3. Comparison between dissociation constant K_d for the couple lysozyme/NAG₃ from literature and the work presented in this paper.

K_d (μM)	Method	Reference
$3 \div 15$	Calorimetry, UV, Fluorescence	[6]
8.6	Fluorescence	[7]
$12 \div 18$	Mass spectroscopy	[8]
10	Mass spectroscopy	[9]
6	Mass spectroscopy	[10]
39.81	Transient induced molecular electronic spectroscopy	[11]
19.6	Mass spectroscopy	[12]
39.8	Mass spectroscopy	[13]
$3 \div 13.7$	(6,5)CNT EGT	this work

REFERENCES

- [1] M. Di Giosia, F. Valle, A. Cantelli, A. Bottoni, F. Zerbetto, E. Fasoli, M. Calvaresi, *Carbon N. Y.* **2019**, *147*, 70.
- [2] D. Schneidman-Duhovny, Y. Inbar, R. Nussinov, H. J. Wolfson, *Nucleic Acids Res.* **2005**, *33*, 363.
- [3] C. Zhang, G. Vasmatzis, J. L. Cornette, C. DeLisi, *J. Mol. Biol.* **1997**, *267*, 707.
- [4] N. Andrusier, R. Nussinov, H. J. Wolfson, *Proteins* **2007**, *69*, 139.
- [5] C. L. Kingsford, B. Chazelle, M. Singh, *Bioinformatics* **2005**, *21*, 1028.
- [6] T. Imoto, L. N. Johnson, A. C. T. North, D. C. Phillips, J. A. Rupley, in *Enzymes*, **1972**, pp. 665–868.
- [7] M. Schindler, N. Sharon, Y. Assaf, D. M. Chipman, *Biochemistry* **1977**, *16*, 423.
- [8] N. Denhart, T. Letzel, *Anal. Bioanal. Chem.* **2006**, *386*, 689.
- [9] C. T. Veros, N. J. Oldham, *Rapid Commun. Mass Spectrom.* **2007**, *21*, 3505.
- [10] S. M. Clark, L. Konermann, *Anal. Chem.* **2005**, *76*, 7077.
- [11] T. Zhang, T. Wei, Y. Han, H. Ma, M. Samieegohar, P. W. Chen, I. Lian, Y. H. Lo, *ACS Cent. Sci.* **2016**, *2*, 834.
- [12] J. Svobodová, S. Mathur, A. Muck, T. Letzel, A. Svatoš, *Electrophoresis* **2010**, *31*, 2680.
- [13] M. C. Jecklin, D. Touboul, C. Bovet, A. Wortmann, R. Zenobi, *J. Am. Soc. Mass Spectrom.* **2008**, *19*, 332.